Initiation, Propagation and Termination in Fluid Phase Free-Radical Polymerization

Michael Buback

Institut für Physikalische Chemie der Georg-August-Universität, Tammannstraße 6, D-37077 Göttingen, Germany

SUMMARY: Free-radical polymerizations are carried out in extended ranges of temperature, pressure, and conversion. The precise knowledge of individual rate coefficients of initiation, propagation, termination, and chain-transfer is essential for the modelling and optimization of monomer conversion and of polymer microstructure in technical polymerizations. In addition to the application-oriented interest, this data is of fundamental importance for the detailed understanding of reaction mechanisms of such free-radical–molecule, free-radical–free-radical, and unimolecular decomposition processes. Even for the polymerization of rather common monomers at moderate temperatures and ambient pressure such information is scarce. The present paper illustrates some recent advances in measuring, within wide ranges of pressure and temperature, propagation and termination rate coefficients of free-radical homo- and copolymerizations and also peroxyester decomposition rate coefficients.

I. Introduction

The advent of laser-assisted techniques has enormously improved the quality by which rate coefficients of elementary reaction steps of free-radical polymerization may be determined. Propagation rate coefficients, k_p, are derived from pulsed-laser induced polymerization (PLP) in conjunction with size-exclusion chromatographic (SEC) analysis of the resulting polymer [1]. The PLP-SEC technique has been used for measuring k_p of several homopolymerizations [2]. Part of these studies has been carried out on polymerizations up to high pressure [3] or in solution [4]. Benchmark values of k_p for styrene, for methyl methacrylate, and for other alkyl methacrylate bulk homopolymerizations have been collated by the IUPAC Working Party „Modeling of Polymerisation Kinetics and Processes" [5]. Termination rate coefficients, k_t,

 CCC 1022-1360/00/$ 17.50+.50/0

are deduced from laser single pulse (SP)-PLP experiments in which monomer conversion induced by one pulse is measured via μs time-resolved near-infrared (NIR) spectroscopy [6]. The method allows for the point-wise probing of k_t as a function of monomer conversion (polymer content) at constant polymerization temperature and pressure. Also via quantitative online vibrational spectroscopy, initiator decomposition rate coefficients may be accurately determined within extended T and p ranges. In Section II of this paper a brief description of two optical high-pressure cells for online spectroscopic analysis will be presented. Selected data from recent PLP-SEC and SP-PLP investigations are contained in Sections III and IV, respectively. In Section V a brief account of quantitative studies into the decomposition rate of alkyl peroxyesters will be given.

II. Optical High Pressure Cells

Vibrational spectroscopic analysis of fluids up to high pressure and temperature including supercritical states has been introduced by Franck and his coworkers [7]. A significant number of IR and NIR modes have been identified, the vibrational intensity of which is only weakly dependent on p and T. This type of behavior enables precise online concentration measurements on fluid systems. Optical cells equipped with windows that are transparent in extended spectral ranges from the IR to the visible and part of the UV region may be used in experiments where both quantitative IR/NIR analysis and UV laser initiation are carried out simultaneously.

The vibrational intensities of IR fundamental and NIR overtone and combination modes mostly differ by orders of magnitudes. Measuring both IR and NIR absorption thus allows to enormously enhance the dynamic range of quantitative spectroscopic analysis. High concentrations, e.g. of starting materials, are recorded with lower sensitivity in the NIR region whereas small concentrations, e.g. of the starting material after almost complete conversion, are monitored via the intense fundamental IR absorption. Thus kinetic data may be collected over an extended conversion range within a single experiment. An overview of optical cells for absorption experiments up to high pressures and temperatures and a detailed description of the experimental procedures has been given elsewhere [8].

Shown in Figure 1 is a basic type of transmission cell for operation up to 500 bar and temperatures up to 300 °C. The probing light penetrates the cell along the cylindrical axis. Each of the windows is mounted on a steel ram with the sealing being achieved according to

Poulter's principle. The pressure at the seating faces exceeds the high pressure inside the cell by the ratio of total surface area of the window to supported area. A spacer of poly(tetrafluorethylene) foil or of gold foil (of about 10 micrometer thickness) is inserted between window and steel ram to compensate for minor imperfections on these polished surfaces. The windows are mostly made from synthetic single-crystalline sapphire or from polycrystalline silicon. In the wavenumber range from 2000 to 50000 cm^{-1}, sapphire is unrivalled as a high-pressure high-temperature window material. The optical path length is determined by the distance between the internal surfaces of the two windows. Sample material is introduced through a hole that is drilled perpendicular to the cylindrical bore. A sheathed thermocouple is housed within another such boring. The optical cell is heated electrically from outside. The cells are made from stainless steel (e.g., German Standard No. 2.4668).

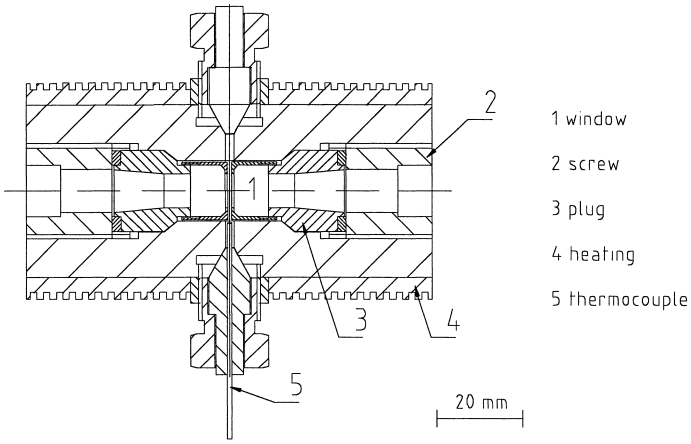

Fig. 1: Optical high-pressure cell for pressures up to 500 bar.

Figure 2 shows an assembly with internal cell. The autoclave may be operated up to 3000 bar and 300 °C, but is constructed according to the same principles as the cell shown in Figure 1. A difference is seen in the way the ram is pressed against the cell body. Whereas a single (central) screw is used with the cell in Figure 1, a flange which is secured by six bolts, is applied with the cell in Figure 2. The internal cell consists of a poly(tetrafluoroethylene) tube, with inner diameter 9 mm and outer diameter 10 mm, and of two cylindrical CaF_2 windows (diameter 10 mm, height 5 mm). The system under investigation is exclusively contained within this internal cell. In addition to effectively avoiding catalytic action of the walls, the

assembly in Figure 2 is perfectly suited for laser-induced experiments as the entire reaction volume is both irradiated by the laser and transmitted by the probing IR or NIR light. Obviously, the assembly in Figure 2 is restricted to batch-type reactions whereas the autoclave without the internal cell (as also the cell in Figure 1) may be used as flow-through cells to monitor concentrations before and/or after passing the reaction medium through a continuously operated reactor.

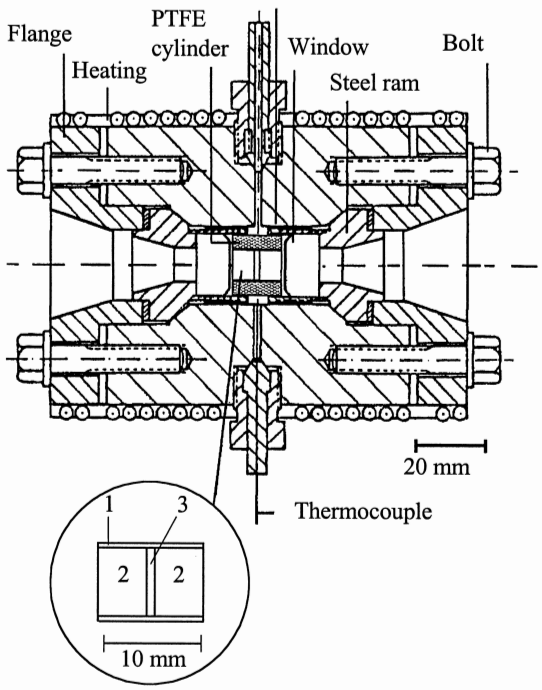

Fig. 2: Optical high-pressure cell with an internal cell consisting of a PTFE tube (1), two CaF_2 windows (2), and the sample volume (3).

III. Propagation Rate Coefficients

The PLP-SEC technique is recommended by the IUPAC Working Party „Modeling of Polymerisation Kinetics and Processes“ as the method of choice for the reliable determination of propagation rate coefficients. An evenly spaced sequence of laser pulses is applied onto the reaction mixture containing (at least) the monomer and a photo-initiator. Polymerization is

run only to low degrees of monomer conversion, typically of 3 per cent. The molecular weight distribution of the resulting polymer is analyzed by size-exclusion chromatography for characteristic inflection points. From the degree of polymerization at these points, the propagation rate coefficient, k_p, is deduced. Actually, the product of propagation rate coefficient and monomer concentration, $k_p \cdot c_M$, is determined. c_M is derived as the arithmetic mean value of the pre-selected initial monomer concentration and the concentration reached after pulsing. It needs to be noted that the overall monomer concentration, c_M, may slightly differ from the microscopic monomer concentration at the site of the free-radical chain end. Although k_p is determined at low degrees of conversion, the obtained propagation rate coefficients apply over rather extended ranges up to moderate and even large conversion. This is due to propagation being chemically controlled.

An essential problem of PLP-SEC investigations relates to the calibration of the MWD which is required for reliably measuring the degree of polymerization at the characteristic points of inflection. Only for a very few homopolymers narrow polydispersity standards are available for a direct SEC calibration. In the majority of cases the principle of universal SEC calibration has to be applied or triple-detector instrumentation has to be used for MWD analysis.

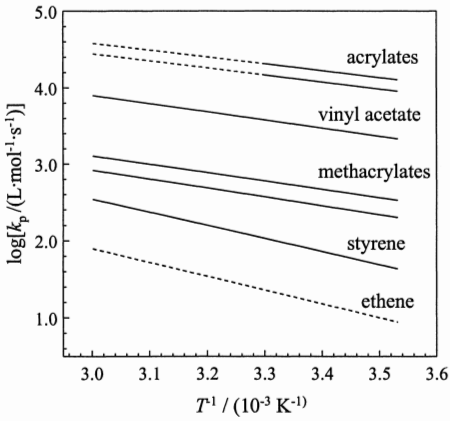

Fig. 3: Temperature dependence of the propagation rate coefficient k_p of several bulk homopolymerizations at ambient pressure. The dashed parts of the Arrhenius lines have been obtained by extrapolation of experimental data taken at other pressure and temperature conditions.

Shown in Figure 3 is an Arrhenius representation of ambient pressure k_p values of several free-radical bulk homopolymerizations. The data has mostly been determined via PLP-SEC. Only the ethene data is from SP-PLP [9]. The dashed parts of the Arrhenius lines indicate that k_p for these conditions has been extrapolated, via measured activation energies and/or activation volumes, from laser-assisted experiments carried out at other polymerization conditions. The ethene data is extrapolated over a fairly large temperature and pressure range,

from above 150°C and 1500 bar, respectively, and are hypothetical in that the free-radical ethene polymerizations may not be carried out at ambient conditions. k_p increases in the series styrene, methacrylates, vinyl acetate, acrylates. For both the acrylates and methacrylates two parallel straight lines are given. They characterize the narrow ranges in which are located the members of the alkyl acrylate family and of the alkyl methacrylate family, respectively. These two families differ appreciably in k_p. Within each family the absolute value of k_p is rather similar (with clear indications of a slight increase in k_p toward larger ester size) and both activation energy and activation volume of k_p can not be distinguished within the limits of experimental accuracy.

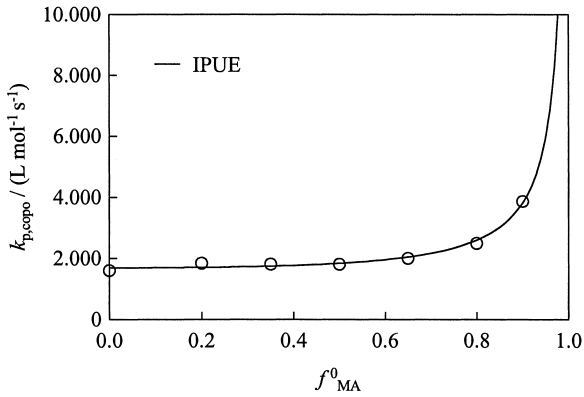

Fig. 4: Propagation rate coefficient, $k_{p,copo}$, of methyl acrylate–dodecyl methacrylate free-radical copolymerizations at 40°C and 1000 bar plotted vs. the (initial) methyl acrylate mole fraction of the monomer mixture.

Figure 4 illustrates copolymerization k_p data determined by Feldermann [10] for the system methyl acrylate (MA) – dodecyl methacrylate (DMA) at 40°C and 1000 bar. The line is a fit of the experimental data to the implicite penultimate unit effect (IPUE) model. That this model is well suited for fitting copolymerization k_p has also been demonstrated for the butyl acrylate (BA) – methyl methacrylate (MMA) system by Hutchinson et al. [11]. The model appears to be applicable to many other free-radical copolymerizations.

Although reactivity ratio (r_i) data have been reported for a large number of copolymerization systems, information on the temperature and pressure dependence of r_i is scarce. In particular for the modelling and optimization of high-pressure high-temperature ethene–(meth)acrylate copolymerizations, accurate data are difficult to obtain. The measurements have to be carried out under extreme conditions. Moreover, the accessible temperature range is rather limited, toward high T by the risk of running into decomposition and toward low T by inhomogeneity of the polymerizing system. As a consequence, the quality of determining the activation

energy associated with r_i is rather poor. It appeared rewarding to try to use kinetic data for low molecular weight free-radical–molecule reactions for an estimate of such activation energies.

The reactivity ratio r_i is defined as the ratio of homo-propagation to cross-propagation rate coefficients of polymeric free radicals ending in species i: $r_i = k_{ii}/ k_{ij}$. The rate coefficients for the addition of monomer to low molecular weight free radicals may not be directly identified with such k_{ii} and k_{ij} values. As propagation steps are chemically controlled, it appears justifiable to use the activation energies of the addition reaction of monomer to low molecular weight free radicals for an estimate of $E_A(r_i)$. A huge number of accurate rate coefficients and of associated activation energies for such addition reactions in liquid solution has been provided by Fischer and his group [12]. The viability of the suggested procedure is illustrated for the copolymerization of ethene and methyl methacrylate in Figure 5.

system		E_A / kJ·mol^{-1}
CH_3·	+ E	28.2 ± 3
	+ MMA	16.0 ± 3
t-Bu-O-CO-C$(CH_3)_2$·	+ E	*38.2 ± 4*
	+ MMA	22.4 ± 3

$$r_i = k_{p,ii} / k_{p,ij} \Rightarrow E_A(r_i) = E_A(k_{p,ii}) - E_A(k_{p,ij})$$

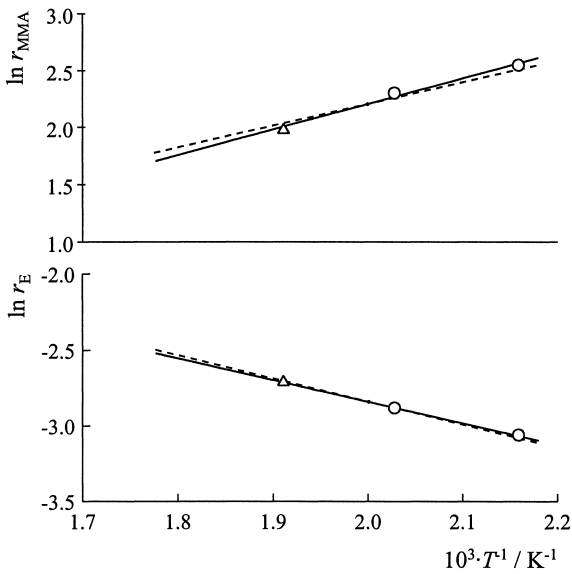

Fig. 5: Arrhenius plots of the measured reactivity ratios of ethene–methyl methacrylate copolymerizations, r_E and r_{MMA}, at 2000 bar. The full line is fitted to the experimental data points (symbols), the slope of the dashed line is derived from the activation energies of addition reactions of the monomers to appropriate small free radicals (see entries in the upper part of the figure and see text).

In the upper part of the figure are listed the activation energies of four addition reactions which appear to be closely related to propagation processes occurring in E–MMA copolymerization. The growing ethylene radical is represented by the methyl radical and the ·C(CH$_3$)$_2$COO*tert*-butyl replaces a growing macro-radical with an MMA terminus. That the latter free radical is indeed a suitable substitute can be seen from the fact that the activation energy for the addition of MMA to ·C(CH$_3$)$_2$COO*tert*-butyl is identical to the experimental activation energy of MMA homopolymerization as derived from PLP-SEC. $r_i = k_{ii}/k_{ij}$ immediately yields $E_A(r_i) = E_A(k_{ii}) - E_A(k_{ij})$. From the tabulated values (upper part of Figure 5) the following numbers are derived: $E_A(r_E) = 12.2 \pm 3$ kJ·mol^{-1} and $E_A(r_{MMA}) = -15.8 \pm 4$ kJ·mol^{-1}. The slope to the dashed lines in Figure 5 is constructed from these calculated activation energies. An excellent agreement is seen with the slope of the line that has been fitted to the experimental data [13].

IV. Termination Rate Coefficients

Free-radical termination is a diffusion-controlled process. Thus significant changes in the termination rate coefficient, k_t, may occur during the course of polymerization reactions where viscosity, e.g. in bulk polymerizations, may vary by several orders of magnitude. Such changes are known to occur in MMA bulk polymerization [14]. In addition, k_t should depend on the chain length of the terminating free radicals. The SP-PLP experiment has turned out to be a powerful tool for investigation of both the conversion and chain-length dependence of termination rate [14, 15]. Recent studies into k_t of several alkyl acrylate and alkyl methacrylate bulk polymerizations showed, that plateau values of almost constant k_t occur in the initial period of these reactions [16]. The region of constant k_t increases toward larger size of the ester group. In MA and MMA polymerizations, k_t stays constant up to conversions between 10 and 20 per cent with the extension of these plateau regions depending on reaction conditions such as pressure, temperature and initiator concentration. With dodecyl acrylate (DA) and with DMA, the plateau k_t value holds up to about 60 per cent monomer conversion. This finding is particularly noteworthy in view of the fact that bulk viscosity decreases within this extended conversion region by several orders of magnitude. Even more remarkable is the observation made by Beuermann et al. [17], that the plateau k_t value (which is insensitive to bulk viscosity) may be shifted significantly by adding a low molecular weight solvent (CO_2)

to the polymerizing system (see also Ref. [16]). The observations are best understood by assigning the initial plateau region to segmental diffusion with this process being controlled by steric hindrance of the terminal and the penultimate units at the free-radical chain end [16, 18]. Toward higher conversion, k_t may become significantly lower than the initial plateau value. Termination is then controlled by translational diffusion and/or by reaction diffusion [14].

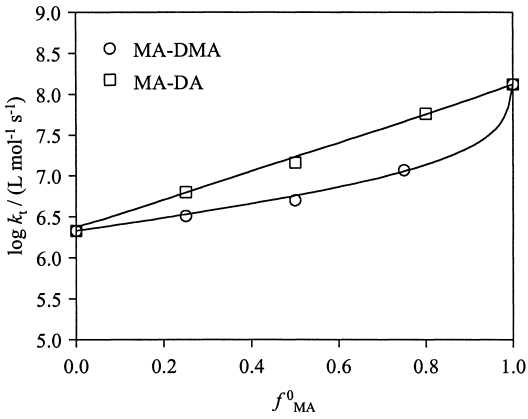

Fig. 6: Termination rate coefficients in the plateau region of MA–DA and MA–DMA copolymerizations at 40°C and 1000 bar plotted vs. the methyl acrylate mole fraction of the (initial) monomer mixture.

Copolymerization experiments turned out to be very helpful with respect to an improved understanding of free-radical termination mechanisms. In Figure 6 are plotted k_t plateau values for MA–DA [18, 19] and MA–DMA [10] copolymerizations at 40°C and 1000 bar vs. the (initial) MA mole fraction of the monomer feed. High-pressure conditions have been chosen for these studies as the signal quality of the SP-PLP experiment largely increases toward high p due to an exponential increase of propagation rate coefficient with pressure. It is not to be expected that different types of dependencies will be seen in case that the experiments are carried out at other p and T conditions. The MA–DA and MA–DMA copolymerization systems are interesting in that the two comonomers to methyl acrylate, DA and DMA, are identical in k_t at this particular p and T condition. The close similarity of DA and DMA k_t's is understood as being due to the steric shielding situation of the large ester groups at the free-radical terminus being the same [18]. The lines are fits of the experimental data to the penultimate unit model for k_t (Eq. 1) in which the unlike (penultimate) rate coefficients $k_{t\,ij,kl}$ are estimated by a geometric mean approximation [20].

$$k_{t\,copo}{}^{0.5} = k_{t\,11,11}{}^{0.5} P_{11} + k_{t\,21,21}{}^{0.5} P_{21} + k_{t\,22,22}{}^{0.5} P_{22} + k_{t\,12,12}{}^{0.5} P_{12} \qquad (1)$$

P_{ij} refers to the relative population of free radicals terminating in unit j with i being the penultimate unit and $k_{t\ ij,ij}$ represents the termination rate coefficient of two free radicals both of which have an ij terminus. Both types of ln k_t vs. f_{MA} behavior are very satisfactorily described by the model underlying Eq. 1. The linear ln k_t vs. f_{MA} dependence seen with the MA–DA system has been discussed in detail in Ref. [19]. The essential reason behind this more or less linear correlation seems to be that both the steric effect and also the intra-coil viscosity follow a simple (linear) logarithmic dependence [16]. Why is the ln k_t vs. f_{MA} relation curved for MA–DMA? The reason for this probably is that the reactivity ratios of the MA–DMA clearly differ from unity (r_{MA} = 0.38 and r_{DMA} = 2.07 [10]). Thus contrary to the situation with MA–DA where both reactivity ratios are close to unity, the populations of the different types of free-radical chain ends are not simply related to f_{MA}. Actually the fraction of free radicals with a methacrylate terminus is higher than the fraction of methacrylate monomer. The model underlying Eq. 1 takes this effect into account in that the actual populations of the different types of free-radical chain ends are introduced. The data in Figure 6 suggest that within one monomer family (associated with reactivity ratios being not too dissimilar from unity) a rather simple, approximately linear dependence of ln k_t on f may be expected whereas in copolymerization of monomers belonging to different families the ln k_t vs. f correlation may be clearly curved (with the exception of trivial situations where the k_t's of the two homopolymerizations are more or less identical). To summarize this argument: Although being different in shape, the two types of ln k_t vs. f behavior depicted in Figure 6 demonstrate that one and the same model (Eq. 1) satisfactorily describes copolymerization k_t. The plateau values of k_t appear to be best understood in terms of termination being controlled by segmental mobility which is primarily affected by steric hindrance at the free-radical site and by the micro-viscosity of the intra-coil medium in which the segmental reorientation takes place [16]. It should be noted that, within the preceding discussion, k_t refers to a chain-length averaged quantity. The potential of measuring the chain-length dependence of k_t is addressed in Ref. [15].

V. Decomposition Rate Coefficients of Peroxyester Initiators

After having addressed termination kinetics and thus free-radical consumption, some aspects of thermal decomposition of peroxides, to provide free radicals, will be briefly discussed.

Online IR-techniques are particularly valuable for such analyses, as will be illustrated for several aliphatic peroxyesters $R(CO)OOC(CH_3)_2R^*$:

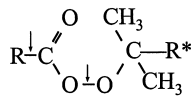

Decomposition rate coefficients should be known for wide p and T ranges, as technical polymerizations are carried out up to 300 °C and 3000 bar. Moreover, information about the decomposition mechanism, via single-bond scission of the O–O bond or via concerted two-bond scission, associated with the immediate formation of CO_2, is required. The latter type of information has important consequences on initiator efficiency and on the type of primary free radicals, oxygen-centered or carbon-centered, which in turn may affect polymeric microstructure, as the two types of free radicals have quite different chain-transfer activities.

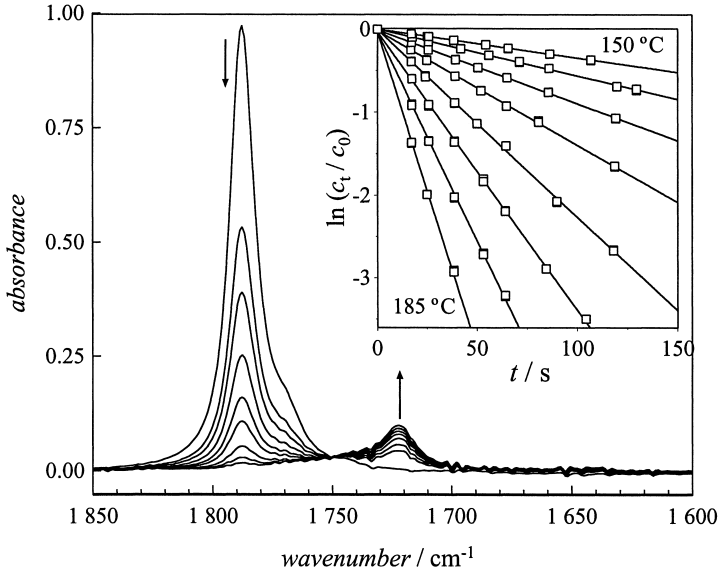

Fig. 7: Infrared absorbance measured in the carbonyl stretching region during the thermal decomposition in *n*-heptane of *tert*-butyl peroxypropionate (TBPProp) at 175°C and 500 bar. The arrows indicate the direction of spectral change with time. Given in the insert are several plots of the time dependence of relative TBPProp concentration, as obtained from spectral series; from the slope to the straight lines the first-order decomposition rate coefficient k_{obs} is obtained [21].

Shown in Figure 7 is a series of IR spectra measured during the course of a *tert*-butyl peroxypropionate (TBPProp ; R = C_2H_5; R* = CH_3) decomposition in *n*-pentane at 500 bar and 175°C [21]. The arrows indicate the direction of spectral changes with reaction time, up to a maximum of 140 s. The decreasing absorption at around 1790 cm^{-1} is due to TBPA. The increasing absorption close to 1722 cm^{-1} comes from acetone that is produced via β - scission of the intermediate *tert*-butoxy free radical. In the insert to Figure 7, the logarithm of relative peroxide concentration, ln (c_t/c_o) is plotted vs. decomposition time t for 500 bar at several temperatures, between 150 and 185°C. For each temperature a straight line is obtained which demonstrates that decomposition is adequately represented by a first-order rate law. The slope to such a linear ln (c_t/c_o) vs. t line yields the first-order decomposition rate coefficient k_{obs}. As has been detailed in Ref. [22], decomposition rate strongly depends on the type of the carbon atom in R that is in α-position to the carbonyl group. In situations where this particular C-atom is primary, k_{obs} is by about one order of magnitude (at temperatures as in Fig. 7) below k_{obs} of the corresponding (with respect to R*) peroxyester with this α - carbon atom being secondary. With this particular carbon atom being tertiary, the decomposition rate is further enhanced, approximately by another factor of ten. The pressure and temperature dependence of k_{obs} clearly indicates that the thermal decomposition of aliphatic peroxyesters occurs via concerted two-bond scission with the above-mentioned α - carbon atom being either secondary or tertiary. The corresponding primary peroxyesters, on the other hand, decompose via single-bond scission.

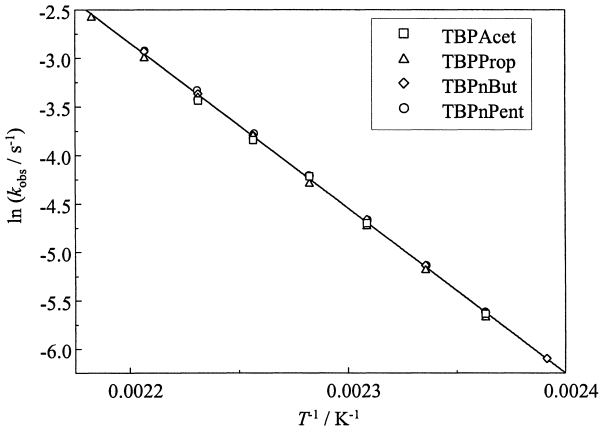

Fig. 8: Arrhenius plot for 500 bar of the decomposition rate coefficient, k_{obs}, of several primary aliphatic *tert*-butyl peroxyesters: *tert*-butyl peroxyacetate (TBPAcet), *tert*-butyl peroxypropionate (TBPProp), *tert*-butyl peroxy-*n*-butyrate (TBP*n*But), and *tert*-butyl peroxy-*n*-pentanoate (TBP*n*Pent) [21, 23].

In Figure 8, decomposition rate coefficients of several such primary aliphatic *tert*-butyl peroxyesters are represented in an Arrhenius plot for 500 bar: *tert*-butyl peroxyacetate (TBPAcet), *tert*-butyl peroxypropionate (TBPProp), *tert*-butyl peroxy-*n*-butyrate (TBP*n*But), and *tert*-butyl peroxy-*n*-pentanoate (TBP*n*Pent) [21, 23]. As can be clearly seen from Figure 8, the rate coefficients for all four „primary" tert-butyl peroxyesters agree within the high experimental accuracy of better than ± 10 %. Extension of the alkyl chain length in R thus is not reflected in the decomposition rate as far as the α - carbon atom in R stays primary.

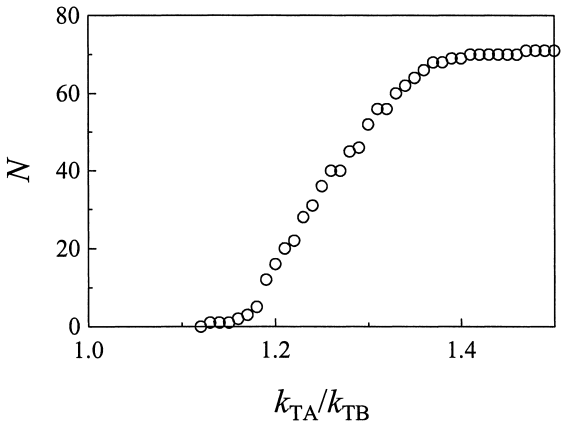

Fig. 9: Ratio of the first-order decomposition rate coefficients of (associated) amyl (R* = C_2H_5) and *tert*-butyl (R* = CH_3) peroxyesters with identical R unit: R = CH_3, $CH(CH_3)_2$, $CH(C_2H_5)C_4H_9$, and $C(CH_3)_3$. The data are from N = 72 independent experiments at temperatures between 100 and 180°C and at pressures between 200 and 2500 bar [24].

Changing the size of the alkyl group in R*, on the other hand has a clear influence on k_{obs}. This is illustrated in Figure 9, where the ratio of decomposition rate coefficients of (associated) amyl (R* = C_2H_5) and *tert*-butyl (R* = CH_3) peroxyesters with identical R unit are plotted: R = CH_3, $CH(CH_3)_2$, $CH(C_2H_5)C_4H_9$, and $C(CH_3)_3$ [24]. Data from N = 72 independent experiments on these „primary", „secondary", and „tertiary" peroxyesters carried out at temperatures between 100 and 180°C and at pressures between 200 and 2500 bar are included in Figure 9. k_{obs} for the amyl peroxyester always exceeds the number for the corresponding rate coefficient of the *tert*-butyl peroxyester. This difference which amounts to 27 ± 9 % and appears to be independent of the type of R unit on the peroxyester, is assigned to steric effects associated with the amyloxy and *tert*-butoxy moieties in the transition state. In going from peroxyacetates (R = CH_3) to peroxypropionates no such entropic effect is seen as the carbonyl group efficiently separates the R group from the reaction site at the O–O bond.

In conclusion: Online vibrational spectroscopic monitoring of kinetics, preferably being carried out in conjunction with laser-assisted techniques allows for the quantitative measurement of rate coefficients that are required for the detailed understanding and modeling of free-radical polymerization processes in extended ranges of pressure and temperature.

Acknowledgements

The author is grateful to the *Deutsche Forschungsgemeinschaft* for support of the research work underlying this survey within the Graduiertenkolleg „Kinetik und Selektivität chemischer Prozesse in verdichteter fluider Phase“ and within the SFB 357 „Molekulare Mechanismen unimolekularer Reaktionen“. The interaction with AKZO NOBEL (in particular with Dr. B. Fischer, Dr. J. Meijer, Dr. A. van Swieten, and R. Gerritsen) in the studies into peroxide decomposition is gratefully acknowledged as is the provision of the peroxide samples. The author is grateful to Dr. S. Beuermann, Dr. H. C. M. van Boxtel, Dipl.-Chem. A. Feldermann, cand.-chem. S. Hinrichs, and Dr. H.-P. Vögele for their support in finalizing this paper.

References

1. O. F. Olaj, I. Bitai, F. Hinkelmann, *Makromol. Chem.* **188**, 1689 (1987); O. F. Olaj, I. Schnöll-Bitai, *Eur. Polym. J.* **25**, 635 (1989)
2. A. M. v. Herk, *J. M. S.-Rev. Macromol. Chem. Phys.* **C37**, 633 (1997)
3. M. Buback, U. Geers, C. H. Kurz, *Macromol. Chem. Phys.* **198**, 3451 (1997); M. Buback, F.-D. Kuchta, *Macromol. Chem. Phys.* **196**, 1887 (1995); S. Beuermann, M. Buback, G. T. Russell, *Macromol. Rapid Commun.* **15**, 351 (1994); M. Buback, C. H. Kurz, C. Schmaltz, *Macromol. Chem. Phys.* **199**, 1721 (1998)
4. S. Beuermann, M. Buback, G. T. Russell, *Macromol. Rapid Commun.* **15**, 647 (1994); M. D. Zammit, T. P. Davis, G. D. Willett, K. F. O'Driscoll, *J. Polym. Sci., Polym. Chem. Ed.* **53**, 2311 (1997); K. F. O'Driscoll, M. J. Monteiro, B. Klumperman, *J. Polym. Sci., Polym. Chem. Ed.* **53**, 515 (1997); R. A. Hutchinson, D. A. Paquet, Jr., S. Beuermann, J. H. McMinn, *Ind. Eng. Chem. Res.* **37**, 3567 (1998)
5. M. Buback, R. G. Gilbert, R. A. Hutchinson, B. Klumperman, F.-D. Kuchta, B. G. Manders, K. F. O'Driscoll, G. T. Russell, J. Schweer, *Macromol. Chem. Phys.* **196**, 3267 (1995); S. Beuermann, M. Buback, T. P. Davis, R. G. Gilbert, R. A. Hutchinson, O. F. Olaj, G. T. Russell, J. Schweer, A. M. van Herk, *Macromol. Chem. Phys.* **198**, 1545 (1997); S. Beuermann, M. Buback, T. P. Davis, R. G. Gilbert, R. A. Hutchinson, A. Kajiwara, B. Klumperman, G. T. Russell, *Macromol. Chem Phys.* **201**, 1355 (2000)
6. M. Buback, H. Hippler, J. Schweer, H.-P. Vögele, *Makromol. Chem., Rapid Commun.* **7**, 261 (1986)

7. E. U. Franck, K. Roth, *Discuss. Faraday Soc.* **43**, 108 (1967); M. Buback, *Angew. Chem., Int. Ed. Engl.* **30**, 641 (1991)
8. M. Buback, C. Hinton, in: *High-pressure techniques in chemistry and physics: a practical approach*, Isaacs and Holzapfel (eds.), Oxford Univ. Press, 1997
9. J. Schweer, *PhD Thesis*, Göttingen 1988
10. A. Feldermann, *Diploma Thesis*, Göttingen 1999
11. R. A. Hutchinson, J. H. McMinn, D. A. Paquet, Jr.; S. Beuermann, C. Jackson, *Ind. Eng. Chem. Res.* **36**, 1103 (1997)
12. H. Fischer in F. Minisci (ed.), *Free Radicals in Biology and Environment*, 63-78, Kluwer Academic Publishers, The Netherlands, 1997; H. Fischer, L. Radom, *Angew. Chem.* (in press)
13. M. Buback, H. Dietzsch, *Macromol. Chem. Phys.* (in press)
14. M. Buback, *Makromol. Chem.* **191**, 1575 (1990)
15. M. Buback, M. Busch, C. Kowollik, *Macromol. Theory Simul.* **9**, 442 (2000)
16. M. Buback, in *Controlled/Living Radical Polymerization*, K. Matyjaszewski, Ed. ACS Symposium Series, 768, Am. Chem. Soc., Washington, 2000, p. 39-56
17. S. Beuermann, M. Buback, C. Isemer, A. Wahl, *Macromol. Rapid Commun.* **20**, 26 (1999)
18. M. Buback, C. Kowollik, *Macromolecules* **32**, 1445 (1999)
19. C. Kowollik, *Free-Radical Bulk Copolymerization Kinetics of Acrylate and Methacrylate Monomers Studied by Pulsed Laser Techniques*, Cuvillier Verlag Göttingen, 1999
20. T. Fukuda, N. Ide, Y.-D. Ma, *Macromol. Symp.* **111**, 305 (1996)
21. J. Sandmann, *PhD Thesis*, Göttingen 2000
22 M. Buback, J. Sandmann, *Z. Phys. Chem (Munich)* **214**, 583 (2000)
23 S. Hinrichs, *Diploma Thesis*, Göttingen 2000
24 M. Buback, D. Nelke, H.-P. Vögele, to be published